

RESEARCH REVIEW

Diagnostic Performance of a Novel Device for Real-Time Margin Assessment in Lumpectomy Specimens

Itzhak Pappo, M.D.,^{*,1} Rona Spector, M.D.,[‡] Asher Schindel, M.D.,[‡] Sara Morgenstern, M.D.,[§] Judith Sandbank, M.D.,[†] Leonor Treho Leider, M.D.,[¶] Shlomo Schneebaum, M.D.,^{||} Shlomo Lelcuk, M.D.,[‡] and Tami Karni, M.D.^{*}

^{*}Department of General Surgery, Assaf Harofeh Medical Center, Zrifin, Israel; [†]Department of Pathology, Assaf Harofeh Medical Center, Zrifin, Israel; [‡]Department of General Surgery, Rabin Medical Center, Beilinson Campus, Petach-Tikva, Israel; [§]Department of Pathology, Rabin Medical Center, Beilinson Campus, Petach-Tikva, Israel; ^{||}Department of General Surgery, Sorasky Medical Center, Tel-Aviv, Israel; and [¶]Department of Pathology, Sorasky Medical Center, Tel-Aviv, Israel

Submitted for publication December 9, 2008

Background. Margin status in breast lumpectomy procedures is a prognostic factor for local recurrence and the need to obtain clear margins is often a cause for repeated surgical procedures. A recently developed device for real-time intraoperative margin assessment (MarginProbe; Dune Medical Devices, Caesarea, Israel), was clinically tested. The work presented here looks at the diagnostic performance of the device.

Methods. The device was applied to freshly excised lumpectomy and mastectomy specimens at specific tissue measurement sites. These measurement sites were accurately marked, cut out, and sent for histopathologic analysis. Device readings (positive or negative) were compared with histology findings (namely malignant, containing any microscopically detected tumor, or nonmalignant) on a per measurement site basis. The sensitivity and specificity of the device was computed for the full dataset and for additional relevant subgroups.

Results. A total of 869 tissue measurement sites were obtained from 76 patients, 753 were analyzed, of which 165 were cancerous and 588 were nonmalignant. Device performance on relatively homogeneous sites was: sensitivity 1.00 (95% CI: 0.85–1), specificity 0.87 (95% CI: 0.83–0.90). Performance for the full dataset was: sensitivity 0.70 (95% CI: 0.63–0.77), specificity 0.70 (95% CI: 0.67–0.74). Device sensitivity was estimated to change from 56% to 97% as the cancer feature size increased from 0.7 mm to 6.6 mm. Detection rate of samples containing pure DCIS clusters was not different from rates of samples containing IDC.

Conclusions. The device has high sensitivity and specificity in distinguishing between normal and cancer tissue even down to small cancer features. © 2010

Elsevier Inc. All rights reserved.

Key Words: breast cancer; dielectric tissue properties; margin status.

INTRODUCTION

The combination of breast conservation surgery with radiation therapy was shown to be equivalent, in terms of survival, to mastectomy for treatment of breast cancer [1]. However, this requires achieving microscopically clean resection margins in the excised lump [2]. While clean margins can be achieved in the initial surgery, re-excision rates reported are between 21% and 50% [3, 4]. In addition to increased costs, morbidity, and poorer cosmetic results, the rate of local recurrence in patients who were re-excised was found to be higher than in those with initial clean margins [5–7]. An investigational device for real-time intraoperative assessment of margin status (MarginProbe; Dune Medical Devices, Caesarea, Israel) has been shown to reduce re-excision rates in breast conservation surgeries by more than 50% by detecting positive margins during the initial excision [8].

This device is based on near-field radio frequency (RF) spectroscopy and is designed to detect differences between dielectric properties of malignant and normal breast tissue adjacent to the probe's sensor. These differences have been studied since the last century and

¹ To whom correspondence and reprint requests should be addressed at The Comprehensive Breast Care Institute, Assaf Harofeh Medical Center, Zerifin 70300, Israel. E-mail: pappo@zahav.net.il.

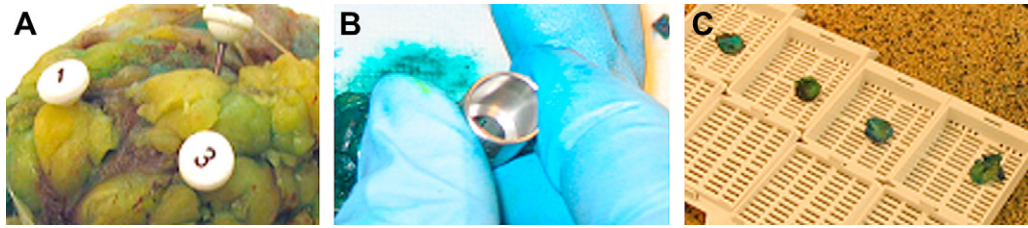


FIG. 1. Tissue handling during the study: (A) breast tissue specimen marking with numbered pins at the center of measurement sites; (B) cutting of a tissue disk around the pin with tissue punch; (C) placement of tissue disks in numbered cassettes. (Color version of figure is available online.)

are well established [9-12]. The differences are a result of changes in ion concentration and mobility, metabolism, water content, membrane and cellular structure, and other characteristics. The device is a single use hand-held tool, connected *via* cables to a console. The hand-held probe is applied to the lumpectomy specimen surface and provides the status of the measurement site in contact with the device tip in real-time. The device does not require intraoperative pathologic analysis.

In this study, we establish the basic diagnostic performance of the device by comparing device output with permanent histopathologic evaluation of the measured tissue sites, sampled on resected breast specimens.

METHODS

General Design

Tissue measurements were performed on freshly excised lumpectomy and mastectomy specimens. All medical staff members were blinded to device output. Measured tissue sites were individually marked, precisely cut out from the main specimen using a biopsy punch, routinely processed, and histologically analyzed.

Eighty patients consented and were enrolled from March 2006 through June 2007 at three medical centers. Inclusion criteria specified female patients over 18 y of age, with diagnosed infiltrative or *in situ* carcinoma of the breast, undergoing lumpectomy or mastectomy. Excluded from this study were patients who underwent neoadjuvant treatment, had prior surgery in the same breast quadrant, or participated in another study.

Device Description

The device used in this work was an investigational diagnostic device (MarginProbe; Dune Medical Devices). The MarginProbe is a near-field RF spectroscopy based real-time detection device, which is designed to distinguish between malignant and non-malignant breast tissue during surgery. It consists of a hand-held single use sterile probe, connected by cables to a console. When the probe tip is placed against tissue it automatically attaches a sensor to the tissue (using a vacuum-based mechanism). The lightweight, hand-held probe applies gentle suction to the tissue for controlled, user-independent attachment. The console sends RF waves over a large frequency range, which are transmitted to the tissue through the sensor. The RF signals are reflected from the tissue through the sensor, and are acquired by the console. The effective measurement volume of the sensor is a 7-mm-diameter disk, up to 1-mm thick. The probe's mechanical footprint is 15 mm in diameter. Each measurement takes approximately 1 to 5 s to complete; thus the probe can be effectively applied to dozens of measurement sites within a few minutes. In this protocol, however, the accurate marking of each measurement

site for subsequent analysis (see description in next section) required more time—approximately 1 min per site. The signals are analyzed in real time, and each measurement is given a positive (malignant), negative (nonmalignant), or a failed result (criteria described below) based on an algorithm that was optimized on a different dataset.

Tissue Measurements and Processing

At the pathology lab, following inking, freshly excised specimens were bread-loafed in order to facilitate access to tumor peripheral measurement sites. The probe was placed in contact with 7-mm wide measurement sites (up to 25 per specimen) on internal surfaces of slices of the specimen, and measurements were taken and recorded. Both grossly cancerous-appearing and normal-appearing measurement sites were sampled. Specific attention was given to the grossly normal appearing sites located close to the tumor. The device readings were logged in the console. All personnel remained blinded to the results during the procedure. In order to ensure accurate correspondence between the tissue site to which the device was applied and that which was histopathologically evaluated, immediately after each measurement the tissue site was marked by a numbered pin placed at the center of the measured area (Fig. 1A). After routine fixation of the specimen (for permanent histopathology analysis), a coin-shaped tissue specimen was cut out from each pinned site using a 10-mm-diameter surgical punch (Fig. 1B), creating 10-mm-diameter tissue disks approximately 2 to 3 mm thick. These tissue samples were placed in cassettes, numbered according to the pin numbers, with the measured side facing a predefined side of the cassette (Fig. 1C). Tissue ink was applied in the hole left by the pin in order to enable the analysis of the measured area (a 7-mm diameter circle concentric to the center pin hole). A slide was prepared for each cassette, parallel to the measured plane. Special care was taken in order to make sure that tissue samples were flat and that each slide contained the full 10-mm circle of tissue, as close as possible to the measured surface (less than 0.5 mm deep).

Data Analysis

Tissue

Each histologic section was microscopically evaluated by a core pathology lab. In addition, slides were digitally scanned and the observed tissue types were marked by the pathologist on the digital images, based on the microscopic analysis of the slide. Within each slide, the pathologist marked all tissue types characterized. These included cancerous types (e.g., invasive ductal carcinoma, ductal carcinoma *in situ*, invasive lobular carcinoma) and numerous nonmalignant types (e.g., mammary, adipose, fibrotic, adenosis, stroma, vascular, lymphatic). Following the digitization of the slides' histopathology data, slides with incomplete histologic data on the full 7-mm circular area measured by the device were disqualified by personnel blinded to device output. Disqualification occurred due to two reasons (defined prior to initiation of the study): (1) an incomplete 7-mm circular shape around the inked pin-hole; (2) unidentifiable inked pin-hole. Beyond these characteristics of disqualified slides no other common features

were present. The coverage area and feature size (denoted as the feature diameter in mm) of the different tissue types were then analyzed automatically by use of dedicated software. Most of the tissue samples contained several tissue types. Sixty-nine percent of the samples contained four or more types and as many as eight types exist in several samples. Following this analysis, each tissue sample was categorized as malignant (if any amount of cancer cells was identified by the pathologist within the 7-mm-diameter circle centered at the inked pin-hole) or nonmalignant.

Measurements

Measurements performed by the device passed automatic qualification tests in real-time by the device software. Two tests are performed: (1) attachment test, based on vacuum levels in the probe acquired during the measurement; and (2) integrity test, checking for any malfunction of the probe in acquiring the RF signal.

All qualified measurements were compared with histology of the tissue samples on a per measurement site basis. Sensitivity and specificity were calculated for the full dataset, as well as for various relevant subsets acquired during the trial. Receiver operating characteristic (ROC) curve analysis was performed on these sets by calculating device output off-line for various algorithm cut-off points and recalculating sensitivities and specificities for each cut-off. In addition, an analysis of sensitivity for various subgroups was performed. Positive measurement sites were divided according to both cancer feature size and according to pathology finding, and the detection rate per subgroup was calculated and compared.

RESULTS

Eighty patients from 3 medical centers were included in the study. Four patients were excluded: two underwent neoadjuvant treatment and for two, a device malfunction occurred and valid data were not obtained. A total number of 869 measurement sites, from 76 patients, were measured and sampled. Of these, 116 (13%) were excluded from this analysis due to incomplete histologic analysis (as noted above). Overall, 753 measurement sites were analyzed.

To assess the device's basic technologic ability, a subset of relatively homogeneous measurement sites was analyzed. The 447 measurement sites in this subset had a single tissue type present in at least 75% of the probe's 7-mm-diameter measurement footprint. Of these 22 (from 15 patients) were cancerous and 425 were nonmalignant. The performance of the device on this dataset was: sensitivity 1.00 (95% CI: 0.85–1), specificity 0.87 (95% CI: 0.83–0.90). For measurement sites containing at least 50% of a single tissue type (29 cancerous, from 18 patients, and 567 nonmalignant) the performance was: sensitivity 1.00 (95% CI: 0.88–1), specificity 0.72 (95% CI: 0.68–0.76). Classification performance on the full dataset (165 cancerous sites from 50 patients, and 588 nonmalignant sites) was: sensitivity 0.70 (95% CI: 0.63–0.77), specificity 0.70 (95% CI: 0.67–0.74).

ROC Curve Analysis

ROC curve presentation of a device's performance can be helpful in the analysis of its diagnostic abilities. Such

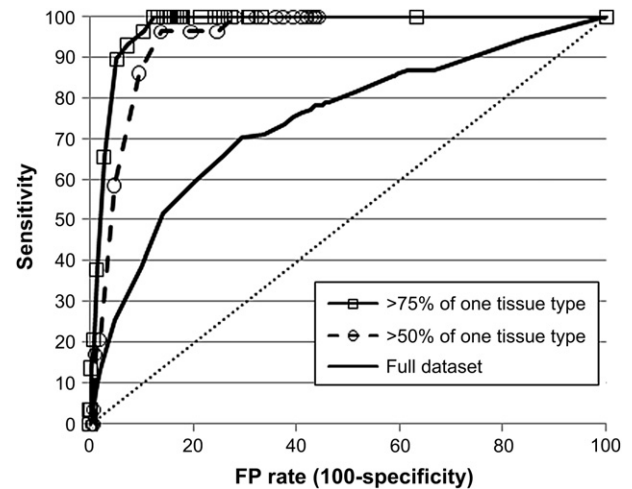


FIG. 2. ROC curves of 3 different datasets: a) samples with >75% content of one tissue type - squares; b) samples with >50% content of one tissue type - circles; and c) full dataset containing all samples - solid line.

a curve plots the sensitivity *versus* the false positive rate (100–specificity) at different cut-off points. **Figure 2** presents ROC curves of the device performance derived by analyzing the data offline and scanning the cutoff point. The figure includes three datasets: (A) tissues containing at least 75% of a single tissue type; (B) all tissues containing at least 50% of a single tissue type; and (C) the full dataset collected in the experiment, containing cancers of all sizes (down to 0.15-mm-diameter features). In addition, **Table 1** summarizes the “areas under graph” (AUG) for each curve with their 95% confidence interval. The dataset containing the most homogeneous tissues, presented in **Fig. 2** by squares, has an AUG of 0.96 (95% CI: 0.94–0.98).

Sensitivity Analysis

In this section, we analyze various subgroups of the cancerous measurement sites. Grouping by cancer feature size and grouping by different cancer histopathology were studied. Note that this analysis has no effect on specificity. In order to assess the performance of the device as the cancerous feature size drops, all the cancerous tissue samples (165) were divided into seven groups according to cancer feature size, and the sensitivity of each group was calculated (**Fig. 3A**). An

TABLE 1
AUG of the ROC Curves in **Fig. 3**

Dataset description	AUG (95% CI: lower–upper)
Tissue samples with >75% content of one tissue type (squares)	0.96 (95% CI: 0.94–0.98)
Tissue samples with >50% content of one tissue type (circles)	0.95 (95% CI: 0.92–0.97)
Full dataset (solid line)	0.74 (95% CI: 0.70–0.79)

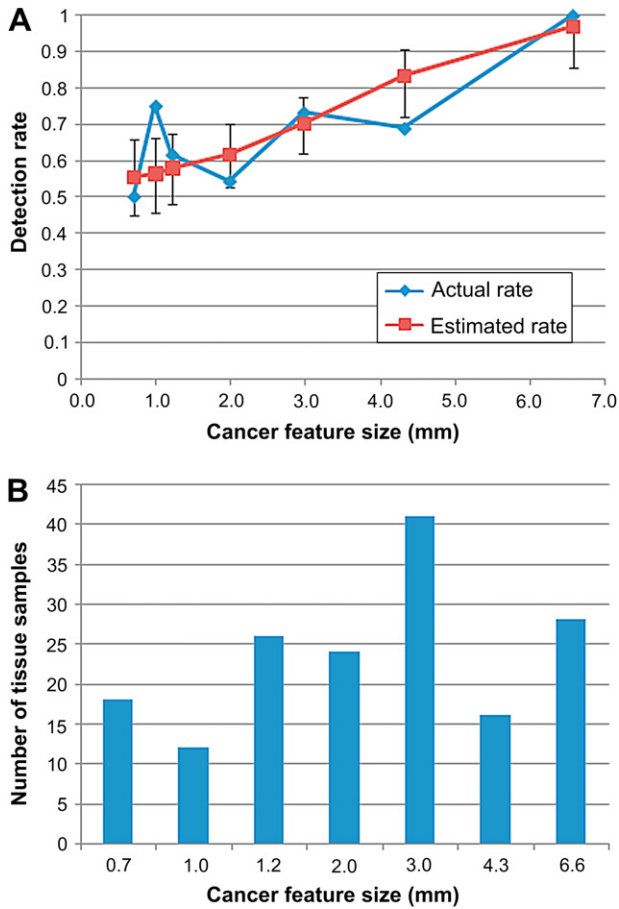


FIG. 3. (A) Detection rate of samples with varying cancer feature size; actual rate in blue and estimated rate (using logistic regression) in red, with estimation error bars denoting 95% confidence levels; (B) histogram of samples per group with average feature size denoted for each group. (Color version of figure is available online.)

estimation of sensitivity as a function of cancer feature size was performed by logistic regression, shown in Fig. 3A, and fits the data well. The number of measurement sites in each group is presented in Fig. 3B and is quite evenly spread. The estimated sensitivity changes from 97% to 56% as the average feature size per group drops from 6.6 mm to 0.7 mm (the group with the average size of 0.7 mm contains cancers of sizes as small as 0.15 mm). All but one of the cancerous samples (28 out of 29) with more than 50% homogeneity belong in the 6.6 mm feature size group, which was detected with sensitivity of 100%. The less homogeneous cancer samples are spread between the various smaller feature size groups. The lower sensitivity in these subgroups brings the overall sensitivity of all the cancer samples to 70%.

It is also of interest to analyze the performance for different histopathology types, irrespective of their feature size. The sensitivity of subgroups divided according to histopathology reporting is summarized in Table 2. No significant differences were observed be-

TABLE 2

Device Sensitivity for Different Histopathology Subgroups: Invasive Ductal Carcinoma (IDC), Ductal Carcinoma *In Situ* (DCIS), Invasive Lobular Carcinoma (ILC), and Combinations of Types. The “Other” Group Includes Rarer Types Such as Mucinous and Papillary Carcinomas

Cancer histopathology	Cancerous samples		
	Number of samples	Detected	Detection rate
IDC	87	59	0.68
DCIS	35	22	0.63
ILC	7	5	0.71
IDC + DCIS	25	21	0.84
ILC + DCIS	3	3	1.00
Other	8	6	0.75
Full dataset	165	116	0.70

tween the subgroups. The two most common groups, invasive ductal carcinoma (IDC) and ductal carcinoma in situ (DCIS), have sensitivities of 0.68 (95% CI:57–77) and 0.63 (95% CI:45–79), respectively.

DISCUSSION

This study shows that the MarginProbe distinguishes between normal and malignant breast tissue with high sensitivity and specificity (100% and 87%, respectively, for relatively homogeneous measurement sites). Device performance decreases for tissues with more heterogeneous compositions. The cancerous samples with high heterogeneity correspond to the small cancer feature sizes. The detection of measurement sites containing very small amounts of malignant tissue was also studied here and the results show a dependence of sensitivity on cancer feature size—as cancer feature size present in the measurement site decreases, so does sensitivity. For features above 5 mm in diameter, the sensitivity is 100%, while taking into account all the malignant tissue measured in the study, down to the smallest feature size (0.15 mm), the sensitivity decreases to 70%. Homogeneity of the nonmalignant tissue samples affects the specificity. While most samples contain several tissue types, in the nonmalignant homogeneous samples containing more than 75% of one tissue type, the coverage area of the other types is much smaller in comparison. However, in the rest of the samples, the coverage area of the various types is evenly spread. The measurements were sampled at locations similar to those that will be encountered by a surgeon during use of the device in the operating room. Thus, the single measurement diagnostic performance presented here is anticipated to hold during

regular use of the device. Since measurements were not taken from the specimen surface, patient-level positive margin analysis was not performed.

The device detection is not limited to invasive cancer malignancy types. More elusive types such as DCIS were detected, with no significant differences in detection rates relative to IDC and other types or combinations of cancer types. The ability to detect DCIS is significant since today DCIS is considered a more challenging intraoperative tissue assessment target.

Device use had no visible effect on the tissue measurement sites nor did it affect the ability to correctly examine samples by permanent histopathology. Ultimately the device is intended to be used intraoperatively to detect positive margins on a specimen surface. It is common practice by surgeons and pathologists to divide the specimen into 6 aspects, and to report margin status for each aspect, subsequently re-excising the corresponding surfaces in the cavity during a second surgery. The device's single measurement site performance, presented here, together with a method for sampling an entire face and a graphical user interface that groups the measurements of each specimen aspect could enable clinical utilization of the device by enabling surgeons to accurately address these positive margins during the first surgery, thus avoiding a second surgery. A recently published study [8] of the device showed reduction of re-excision rates by more than 50% by using the device for detection of positive margins during the initial excision. Further studies of the clinical utility of the device are underway.

REFERENCES

1. Fisher B, Anderson S, Bryant J, et al. Twenty-year follow-up of a randomized trial comparing total mastectomy, lumpectomy, and lumpectomy plus irradiation for the treatment of invasive breast cancer. *N Engl J Med* 2002;347:1233;
2. Veronesi U, Cascinelli N, Mariani L, et al. Twenty-year follow-up of a randomized study comparing breast-conserving surgery with radical mastectomy for early breast cancer. *N Engl J Med* 2002;347:1227.
3. NCCN Clinical Practice Guidelines in Oncology™. National Comprehensive Cancer Network, 2007.
4. Tafra L, Fine R, Whitworth P, et al. Prospective randomized study comparing cryo-assisted and needle-wire localization of ultrasound visible breast tumors. *Am J Surg* 2006;192:462.
5. Menes TS, Tartter PI, Bleiweiss I, et al. The consequence of multiple re-excisions to obtain clear lumpectomy margins in breast cancer patients. *Ann Surg Oncol* 2005;12:881.
6. Aziz D, Rawlinson E, Narod SA, et al. The role of re-excision for positive margins in optimizing local disease control after breast-conserving surgery for cancer. *Breast J* 2006;12:331.
7. Tartter PI, Kaplan J, Bleiweiss I, et al. Lumpectomy margins, re-excision, and local recurrence of breast cancer. *Am J Surg* 2000; 179:81.
8. Anscher MS, Jones P, Prosnitz LR, et al. Local failure and margin status in early-stage breast carcinoma treated with conservation surgery and radiation therapy. *Ann Surg* 1993;218:22.
9. Allweiss TM, Kaufman Z, Lelcuk S, et al. A prospective, randomized, controlled, multicenter study of a real-time, intraoperative probe for positive margin detection in breast-conserving surgery. *Am J Surg* 2008;196:483.
10. Gabriel S, Lau RW, Gabriel C. The dielectric properties of biological tissue II: Measurements in the frequency range 10 Hz to 20 GHz. *Phys Med Biol* 1996;41:2251.
11. Foster KR, Schepps JL. Dielectric properties of tumor and normal tissues at radio through microwave frequencies. *J Microw Power* 1981;16:107.
12. Morimoto T, Kimura S, Konishi Y, et al. A study of the electrical bio-impedance of tumors. *J Inv Surg* 1993;6:25.
13. Joines WT, Zhang Y, Li C, et al. The measured electrical properties of normal and malignant human tissues from 50 to 900 MHz. *Med Phys* 1994;21:547.